

New Ru(II) Chromophores with Extended Excited-State Lifetimes

Daniel S. Tyson, Charles R. Luman, Xiaoli Zhou, and Felix N. Castellano*

Department of Chemistry and Center for Photochemical Sciences, Bowling Green State University, Bowling Green, Ohio 43403

Received March 15, 2001

We describe the synthesis, electrochemical, and photophysical properties of two new luminescent Ru(II) diimine complexes covalently attached to one and three 4-piperidinyl-1,8-naphthalimide (PNI) chromophores, [Ru(bpy)₂(PNI-phen)](PF₆)₂ and [Ru(PNI-phen)₃](PF₆)₂, respectively. These compounds represent a new class of visible light-harvesting Ru(II) chromophores that exhibit greatly enhanced room-temperature metal-to-ligand charge transfer (MLCT) emission lifetimes as a result of intervening intraligand triplet states (³IL) present on the pendant naphthalimide chromophore(s). In both Ru(II) complexes, the intense singlet fluorescence of the pendant PNI chromophore(s) is nearly quantitatively quenched and was found to sensitize the MLCT-based photoluminescence. Excitation into either the ¹IL or ¹MLCT absorption bands results in the formation of both ³MLCT and ³IL excited states, conveniently monitored by transient absorption and fluorescence spectroscopy. The relative energy ordering of these triplet states was determined using time-resolved emission spectra at 77 K in an EtOH/MeOH glass where dual emission from both Ru(II) complexes was observed. Here, the shorter-lived higher energy emission has a spectral profile consistent with that typically observed from ³MLCT excited states, whereas the millisecond lifetime lower energy band was attributed to ³IL phosphorescence of the PNI chromophore. At room temperature the data are consistent with an excited-state equilibrium between the higher energy ³MLCT states and the lower energy ³PNI states. Both complexes display MLCT-based emission with room-temperature lifetimes that range from 16 to 115 μs depending upon solvent and the number of PNI chromophores present. At 77 K it is apparent that the two triplet states are no longer in thermal equilibrium and independently decay to the ground state.

Introduction

The photochemical and photophysical properties of compounds containing d⁶ transition metals, particularly those based on Ru(II), continue to receive considerable attention.¹ This is

largely due to the potential applications of these chromophores in diverse areas such as solar energy conversion,² luminescence sensing,^{3,4} biotechnology,⁵ electroluminescence displays,^{6,7} and photochemical molecular devices.⁸ In most cases, photoluminescence is generally observed from only one state in Ru(II) diimine complexes displaying metal-to-ligand charge transfer (MLCT) excited states. In other instances, some complexes possess MLCT excited states that coexist with intraligand (IL) or ligand-localized triplet excited states that can interact strongly or weakly depending upon the relative ordering of the energy levels in the participating excited states.⁹ In this genre of chromophores, there are several examples of strongly interacting systems that attain thermal equilibrium in the triplet manifold. To date these systems have been based on Ru(II)-pyrene complexes containing a variety of covalent linkages between the two chromophores.^{10–13} This interaction generates com-

* To whom correspondence should be sent. Fax: (419) 372-9809. E-mail: castell@bgsu.edu

- (1) For reviews of MLCT excited states: (a) Juris, A.; Balzani, V.; Barigelletti, F.; Campagna, S.; Belser, P.; von Zelewsky, A. *Coord. Chem. Rev.* **1988**, *84*, 85. (b) Meyer, T. J. *Acc. Chem. Res.* **1989**, *22*, 1048. (c) Demas, J. N.; DeGraff, B. A. *Anal. Chem.* **1991**, *63*, 829A. (d) Kalyanasundaram, K. *Photochemistry of Polypyridine and Porphyrin Complexes*; Academic Press: San Diego, 1992. (e) Roundhill, D. M. *Photochemistry and Photophysics of Metal Complexes*; Plenum Press: New York, 1994. (f) *Organic and Inorganic Photochemistry*; Ramamurthy, V., Schanze, K. S., Eds.; M. Dekker: New York, 1998.
- (2) (a) O'Regan, B.; Grätzel, M. *Nature* **1991**, *353*, 737. (b) *Photosensitization and Photocatalysis Using Inorganic and Organometallic Compounds*; Kalyanasundaram, K., Grätzel, M., Eds. Kluwer: Dordrecht, 1993.
- (3) (a) *Topics in Fluorescence Spectroscopy, Vol. 4: Probe Design and Chemical Sensing*; Lakowicz, J. R., Ed.; Plenum Press: New York, 1994. (b) Szmecinski, H.; Lakowicz, J. R., *Sensors Actuators B* **1995**, *29*, 16. (c) Castellano, F. N.; Lakowicz, J. R. *Photochem. Photobiol.* **1998**, *67*, 179. (d) Lakowicz, J. R.; Castellano, F. N.; Dattelbaum, J. D.; Tolosa, L.; Rao, G.; Gryczynski, I. *Anal. Chem.* **1998**, *70*, 5115.
- (4) (a) de Silva, A. P.; Gunaratne, H. Q.; Gunnlaugsson, T.; Huxley, A. J. M.; McCoy, C. P.; Rademacher, J. T.; Rice, T. E. *Chem. Rev.* **1997**, *97*, 1515. (b) Slone, R. V.; Benkstein, K. D.; Belanger, S.; Hupp, J. T.; Guzei, I. A.; Rheingold, A. L. *Coord. Chem. Rev.* **1998**, *171*, 221. (c) Beer, P. D. *Acc. Chem. Res.* **1998**, *31*, 71. (d) Sun, S.-S.; Lees, A. J. *Chem. Commun.* **2000**, 1687. (e) Demas, J. N.; DeGraff, B. A. *Coord. Chem. Rev.* **2001**, *211*, 317.
- (5) (a) Terpetschnig, E.; Szmecinski, H.; Malak, H.; Lakowicz, J. R. *Biophys. J.* **1995**, *68*, 342. (b) Guo, X.-Q.; Castellano, F. N.; Li, L.; Lakowicz, J. R. *Anal. Chem.* **1998**, *70*, 632.
- (6) (a) Gao, F. G.; Bard, A. J. *J. Am. Chem. Soc.* **2000**, *122*, 7426. (b) Elliott, C. M.; Pichot, F.; Bloom, C. J.; Rider, L. S. *J. Am. Chem. Soc.* **1998**, *120*, 6781.
- (7) (a) Lee, J.-K.; Yoo, D.; Rubner, M. F. *Chem. Mater.* **1997**, *9*, 1710. (b) Lyons, C. H.; Abbas, E. D.; Lee, J.-K.; Rubner, M. F. *J. Am. Chem. Soc.* **1998**, *120*, 12100. (c) Handy, E. S.; Pal, A. J.; Rubner, M. F. *J. Am. Chem. Soc.* **1999**, *121*, 3525. (d) Wu, A.; Yoo, D.; Lee, J.-K.; Rubner, M. F. *J. Am. Chem. Soc.* **1999**, *121*, 4883.
- (8) (a) Balzani, V.; Scandola, F. *Supramolecular Photochemistry*; Horwood: Chichester, 1991. (b) Lehn, J.-M. *Supramolecular Chemistry: Concepts and Perspectives*; VCH: Weinheim, 1995.
- (9) Baba, A. I.; Shaw, J. R.; Simon, J. A.; Thummel, R. P.; Schmehl, R. H. *Coord. Chem. Rev.* **1998**, *171*, 43.
- (10) Ford, W. E.; Rodgers, M. A. J. *J. Phys. Chem.* **1992**, *96*, 2917.
- (11) (a) Wilson, G. J.; Sasse, W. H. F.; Mau, A. W. H. *Chem. Phys. Lett.* **1996**, *250*, 583. (b) Wilson, G. J.; Launikonis, A.; Sasse, W. H. F.; Mau, A. W. H. *J. Phys. Chem. A* **1997**, *101*, 4860. (c) Wilson, G. J.; Launikonis, A.; Sasse, W. H. F.; Mau, A. W. H. *J. Phys. Chem. A* **1998**, *102*, 5150.
- (12) (a) Harriman, A.; Hissler, M.; Khatyr, A.; Ziessel, R. *Chem. Commun.* **1999**, 735. (b) Hissler, M.; Harriman, A.; Khatyr, A.; Ziessel, R. *Chem. J. Eur.* **1999**, *5*, 3366.

pounds exhibiting lifetimes that greatly exceed those normally observed in MLCT complexes. In addition, there exist other cases where the $^3\text{MLCT}$ and ^3IL states weakly interact and independently relax to the ground state. As far as the latter are concerned, only a few examples of mononuclear Ru(II) complexes that exhibit two nonequilibrated excited states at room temperature have been reported to date.^{14,15} As convincingly demonstrated by Schmehl and co-workers,¹⁴ such molecules can also display greatly enhanced excited-state lifetimes. Although both classes of metal complexes with coexisting $^3\text{MLCT}$ and ^3IL states are intrinsically different, they each provide a pathway for the extension of excited-state lifetimes. Many potential applications requiring extended lifetimes will likely be insensitive to how these lifetimes are actually achieved. Therefore further development of new complexes that concurrently exhibit $^3\text{MLCT}$ and ^3IL excited states seems appropriate.

The present study merges our recent research interests in metal-organic light-harvesting chromophores and MLCT compounds with extended lifetimes.^{13,16} Specifically, a 4-piperidinyl-1,8-naphthalimide (PNI) chromophore was covalently attached to the 5-position of 1,10-phenanthroline (PNI-phen) which was used to prepare two new Ru(II) complexes, incorporating one (dyad) and three (tetrad) PNI units to give $[\text{Ru}(\text{bpy})_2(\text{PNI-phen})](\text{PF}_6)_2$ and $[\text{Ru}(\text{PNI-phen})_3](\text{PF}_6)_2$, respectively. The visible-absorbing PNI dye displays intense singlet fluorescence in a variety of solvents which overlaps the Ru(II) MLCT absorption transitions in the visible, favorable for efficient Förster-type resonance energy transfer.^{16b,17,18} Interestingly, the PNI chromophores possess low-lying triplet states that are nearly isoenergetic, but lower in energy, with respect to the $^3\text{MLCT}$ states present in each complex. Excitation of either the ^1PNI or $^1\text{MLCT}$ absorption bands results in population of both the ^3PNI and $^3\text{MLCT}$ excited states, conveniently monitored using a variety of spectroscopic techniques. At room temperature in a variety of solvents, the emission emerges as MLCT-based luminescence possessing lifetimes ranging from 16 to 115 μs , which is substantially quenched in the presence of dioxygen (to less than 200 ns). Our experimental observations are consistent with the establishment of a thermally equilibrated excited state between the $^3\text{MLCT}$ and the ^3PNI states at room temperature, similar to that previously observed in several Ru(II)-pyrenyl chromophores.¹⁰⁻¹³ At 77 K the triplet equilibrium was no longer established and dual emission from the $^3\text{MLCT}$ and ^3PNI states was observed using time-resolved emission spectroscopy. From the time-resolved spectra, we were able to make definitive assignments regarding the triplet energy levels of both chromophores present in each molecule without having to rely on data from model systems. This work represents the first observation of triplet excited-state equilibrium in a Ru(II) complex without incorporating pyrene.

Experimental Section

Chemicals. All synthetic manipulations were performed under an inert and dry argon atmosphere using standard techniques. Piperidine, *p*-toluidine, 2,2'-bipyridine (bpy), 1,10-phenanthroline (phen), thioxanthene-9-one (thioxanthone), 1,4-diazobicyclo[2.2.2]octane (DABCO), and 4-nitronaphthalene-1,8-dicarboxyanhydride were obtained from Aldrich and used as received. 5-Amino-1,10-phenanthroline was purchased from Polysciences and used without further purification. Electrochemical grade tetrabutylammonium perchlorate (TBAP) was obtained from the G. F. Smith Chemical Company and was used as received. Water was deionized with a Barnstead E-Pure system. Absolute ethanol and DMF were dried and distilled prior to use. All other reagents were obtained from commercial sources and used as received. $\text{Ru}(\text{bpy})_2\text{Cl}_2$ and $\text{Ru}(\text{DMSO})_4\text{Cl}_2$ were prepared according to published procedures.^{19,20} $[\text{Ru}(\text{bpy})_2(\text{phen})]^{2+}$ and $[\text{Ru}(\text{phen})_3]^{2+}$ were prepared and purified in the same manner as the dyad and tetrad described below using phen in place of PNI-phen. *N*-(4-methylphenyl)-4-nitronaphthalene-1,8-dicarboximide (**1**) and *N*-(4-methylphenyl)-4-(1-piperidinyl)naphthalene-1,8-dicarboximide (**2**) were prepared following literature methods, yielding satisfactory ^1H NMR and mass spectra.^{21a} Commercially available $[\text{Ru}(\text{bpy})_3]\text{Cl}_2 \cdot 6\text{H}_2\text{O}$ (Aldrich) was converted into the corresponding PF_6^- salt by metathesis with NH_4PF_6 (Aldrich) in water.

***N*-(1,10-Phenanthroline)-4-nitronaphthalene-1,8-dicarboximide (**3**).** 4-Nitronaphthalene-1,8-dicarboxyanhydride (374 mg, 1.54 mmol) and 5-amino-1,10-phenanthroline (300 mg, 1.54 mmol) were refluxed in anhydrous ethanol (50 mL) for 2 days, upon which the product precipitated. Once cool, petroleum ether at 0 °C was added to promote further crystallization. The light tan solid was collected on a fine glass frit and rinsed with chilled ethanol and petroleum ether to afford the title compound in 53% yield, which was used without further purification. This compound decomposes above 241 °C. ^1H NMR (CDCl_3): δ 9.25 (m, 2H), 8.95 (d, 1H), 8.80 (t, 2H), 8.47 (d, 1H), 8.29 (dd, 1H), 7.97–8.12 (m, 2H), 7.88 (s, 1H), 7.70 (dd, 1H), 7.58 (dd, 1H). EI-MS: m/z 420 (M^+).

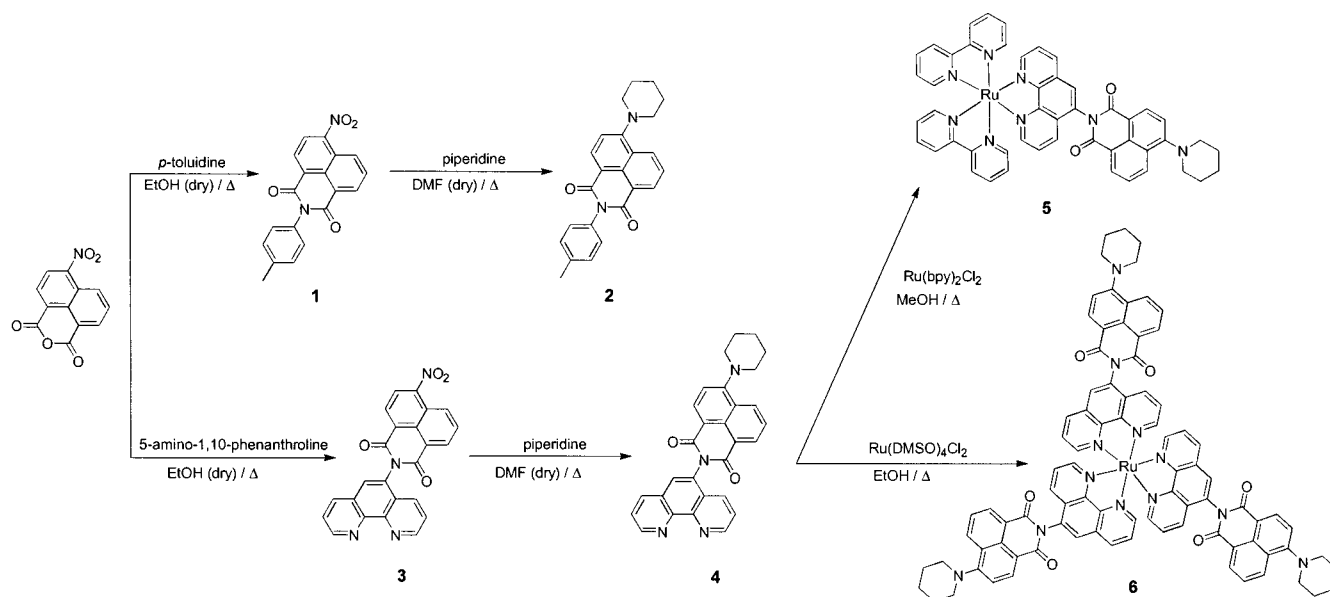
***N*-(1,10-Phenanthroline)-4-(1-piperidinyl)naphthalene-1,8-dicarboximide (PNI-phen), (**4**).** *N*-(1,10-Phenanthroline)-4-nitronaphthalene-1,8-dicarboximide (460 mg, 1.10 mmol) and piperidine (541 μL , 5.47 mmol) were refluxed in anhydrous DMF (10 mL) for 2 h. Once cool, the reaction mixture was poured into CH_2Cl_2 (100 mL) and washed twice with water, dried over MgSO_4 , and rotary evaporated to a dark residue. The residue was dissolved in a minimum amount of dry CH_2Cl_2 and slowly dripped into cold petroleum ether. The yellow precipitate was collected on a fine glass frit and rinsed with cold petroleum ether. The title compound was obtained in 61% yield and used without further purification. Mp: >260 °C. ^1H NMR (CDCl_3): δ 9.26 (m, 2H), 8.50–8.68 (m, 3H), 8.30 (d, 1H), 8.06 (d, 1H), 7.89 (s, 1H), 7.67–7.81 (m, 3H), 7.58 (dd, 1H), 3.32 (m, 4H), 1.85 (bm, 6H). EI-MS: m/z 458 (M^+).

Bis(2,2'-bipyridine)(*N*-(1,10-phenanthroline)-4-(1-piperidinyl)-naphthalene-1,8-dicarboximide)ruthenium(II)hexafluorophosphate, $[\text{Ru}(\text{bpy})_2(\text{PNI-phen})](\text{PF}_6)_2$ (5**).** $\text{Ru}(\text{bpy})_2\text{Cl}_2$ (15.5 mg, 0.030 mmol) and **4** (15.0 mg, 0.033 mmol) were suspended in methanol (40 mL), protected from light, and refluxed for 3 h while stirring. The reaction solution was cooled to room temperature, water (10 mL) was added, and the solution filtered. Dropwise addition of 20 mL saturated NH_4PF_6 (aq) generated an orange precipitate. The solid was collected by filtration through a fine glass frit and washed with water, followed by diethyl ether to afford the crude product. The title compound was

- (13) (a) Tyson, D. S.; Castellano, F. N. *J. Phys. Chem. A* **1999**, *103*, 10955. (b) Tyson, D. S.; Bialecki, J.; Castellano, F. N. *Chem. Commun.* **2000**, 2355.
- (14) Simon, J. A.; Curry, S. L.; Schmehl, R. H.; Schatz, T. R.; Piotrowiak, P.; Jin, X.; Thummel, R. P. *J. Am. Chem. Soc.* **1997**, *119*, 11012.
- (15) (a) Shaw, J. R.; Webb, R. T.; Schmehl, R. H. *J. Am. Chem. Soc.* **1990**, *112*, 1117. (b) Baba, A. I.; Ensley, H. E.; Schmehl, R. H. *Inorg. Chem.* **1995**, *34*, 1198. (c) Taffarel, E.; Chirayil, S.; Kim, W.; Thummel, R.; Schmehl, R. H. *Inorg. Chem.* **1996**, *35*, 2127.
- (16) (a) Tyson, D. S.; Castellano, F. N. *Inorg. Chem.* **1999**, *38*, 4382. (b) Tyson, D. S.; Gryczynski, I.; Castellano, F. N. *J. Phys. Chem. A* **2000**, *104*, 2919. (c) Zhou, X.; Tyson, D. S.; Castellano, F. N. *Angew. Chem., Int. Ed.* **2000**, *39*, 4301.
- (17) (a) Förster, T. *Ann. Phys. (Leipzig)* **1948**, *2*, 55. (b) Förster, T. *Z. Naturforsch* **1949**, *4a*, 321. (c) Förster, T. *Discuss. Faraday Soc.* **1959**, *27*, 7.
- (18) Lakowicz, J. R. *Principles of Fluorescence Spectroscopy*, 2nd ed.; Kluwer Academic/Plenum Publishers: New York, 1999.

- (19) Sullivan, B. P.; Salmon, D. J.; Meyer, T. J. *Inorg. Chem.* **1978**, *17*, 3334.
- (20) Evans, I. P.; Spencer, A.; Wilkinson, G. J. *J. Chem. Soc., Dalton Trans.* **1973**, 204.
- (21) (a) Greenfield, S. R.; Svec, W. A.; Gosztola, D.; Wasielewski, M. R. *J. Am. Chem. Soc.* **1996**, *118*, 6767. (b) de Silva, P.; Quaranté, N.; Habib-Jiwani, J.-L.; McCoy, C. P.; Rice, T. E.; Soumillion, J.-P. *Angew. Chem., Int. Ed. Engl.* **1995**, *34*, 1728. (c) Alexiou, M. S.; Tychopoulos, V.; Ghorbanian, S.; Tyman, J. H. P.; Brown, R. G.; Brittain, P. I. *J. Chem. Soc., Perkin Trans. 2* **1990**, 837. (d) Middleton, R. W.; Parrick, J.; Clarke, E. D.; Wardman, P. J. *Heterocycl. Chem.* **1986**, *23*, 849.

Scheme 1



purified by chromatography on Sephadex LH-20 (25 × 2 cm, CH₃OH) and crystallized by addition of concentrated NH₄PF₆ (aq). The yield was 34% after purification. FAB-MS: *m/z* 1017.6 [M⁺ - PF₆], 872.5 [M⁺ - 2PF₆].

Tris(*N*-(1,10-phenanthroline)-4-(1-piperidinyl)naphthalene-1,8-dicarboximide)ruthenium(II)hexafluorophosphate, [Ru(PNI-phen)₃](PF₆)₂ (6). Ru(DMSO)₄Cl₂ (27.5 mg, 0.057 mmol) and **4** (85.7 mg, 0.187 mmol) were dissolved in 95% ethanol (10 mL), protected from light, and refluxed for 24 h. Once the solution was cooled to room temperature, 5 mL water was added, and the mixture filtered. Aqueous NH₄PF₆ was added and a dark orange solid immediately precipitated. The solid was collected on a fine glass frit and washed with water and ether to afford the crude product. The complex was purified by chromatography on Sephadex LH-20 (25 × 2 cm, CH₃OH) and crystallized by addition of concentrated NH₄PF₆ (aq). After purification the yield was 45%. FAB-MS: *m/z* 1621 [M⁺ - PF₆], 1477 (M⁺ - 2PF₆).

General Techniques. ¹H NMR spectra were recorded on a Varian Gemini 200 (200 MHz) spectrometer. All chemical shifts were referenced to residual solvent signals previously referenced to TMS. FAB mass spectra were measured at the University of Maryland College Park Mass Spectrometry Laboratory. DIP mass spectra were obtained using a Shimadzu QP5050A mass spectrometer. Absorption spectra were measured with a Hewlett-Packard 8453 diode array spectrophotometer. Static luminescence spectra were obtained with a single photon counting spectrofluorimeter from Edinburgh Analytical Instruments (FL/FS 900). Excitation spectra were corrected with a photodiode mounted inside the fluorimeter that continuously measures the Xe lamp output. This instrument was also utilized for time-correlated single photon counting (TCSPC) experiments. The excitation source for the TCSPC measurements was a nanosecond flashlamp operating under an atmosphere of H₂ gas (0.50–0.55 bar, 1.2 ns fwhm, 40 kHz repetition rate), whose output was filtered through a monochromator prior to sample excitation. TCSPC data were analyzed by iterative convolution of the luminescence decay profile with the instrument response function using software provided by Edinburgh Instruments.

Emission lifetimes were also measured with a nitrogen-pumped broadband dye laser (2–3 nm fwhm) from PTI (GL-3300 N₂ laser, GL-301 dye laser), using an apparatus that has been previously described.^{13a} Coumarin 460 (440–480 nm) and Coumarin 500 (490–550 nm) laser dyes were used to tune the unfocused excitation. Pulse energies were typically attenuated to ~100 μJ/pulse, measured with a Moletron Joulemeter (J4-05). This apparatus was also used to measure time-resolved emission spectra following dye laser excitation.

All fluorescence and luminescence experiments used optically dilute solutions (OD ~0.1) prepared in spectroscopic grade solvents. Transient

absorption samples were maintained at 0.2 OD at the excitation wavelength. Radiative quantum yields (Φ_r) of each metal complex were measured relative to [Ru(bpy)₃](PF₆)₂ for which Φ_r = 0.062 in CH₃CN, accurate to 10%.²² Fluorescence quantum yields were measured relative to PNI in toluene (Φ_r = 0.91).^{21a} Frozen glass emission samples at 77 K were prepared by inserting a 5 mm (internal diameter) NMR tube containing a 10⁻⁵ M solution (4:1 EtOH/MeOH) of the appropriate compound into a quartz-tipped finger dewar of liquid nitrogen. In some instances, 10% ethyl iodide was added to induce phosphorescence.

Nanosecond time-resolved absorption spectroscopy was performed using instrumentation that has been described previously.^{13a,23} Briefly, the excitation source was the unfocused second or third harmonic (532 or 355 nm, 5–7 ns fwhm) output of a Nd:YAG laser (Continuum Surelite I). Typical excitation energies were maintained at 10 mJ/pulse. Samples were continuously purged with a stream of high purity argon or nitrogen gas throughout the experiments. The data, consisting of a 10-shot average of both the signal and the baseline, were analyzed with programs of local origin. All transient absorption measurements were conducted at the ambient temperature, 22 ± 2 °C. Long-term exposure of certain samples to flash photolysis resulted in minor decomposition, thus fresh samples were used for each experiment.

Electrochemical potentials were obtained in acetonitrile solutions containing 2 mM analyte and 0.1 M TBAP as supporting electrolyte. Solutions were bubbled with argon prior to each measurement. A Bioanalytical Systems Epsilon controller interfaced with a Pentium PC was used to obtain the cyclic voltammetry data. A platinum disk working electrode, platinum wire auxiliary electrode, and a Ag/AgCl (3M KCl) reference electrode were used for all measurements. A scan rate of 200 mV/s was typically employed. Under these experimental conditions the ferrocene/ferrocenium couple was determined to be +0.44 V vs Ag/AgCl.

Results

Syntheses. The ligand *N*-(1,10-phenanthroline)-4-(1-piperidinyl)naphthalene-1,8-dicarboximide (PNI-phen, **4**) and the model compound *N*-(4-methylphenyl)-4-(1-piperidinyl)naphthalene-1,8-dicarboximide (PNI, **2**) were prepared using well-established synthetic protocols (Scheme 1).²¹ Reaction of 4-nitronaphthalene-1,8-dicarboxyanhydride with *p*-toluidine or 5-amino-1,10-phenanthroline in refluxing ethanol yields the

(22) Caspar, J. V.; Meyer, T. J. *J. Am. Chem. Soc.* **1983**, *105*, 5583.

(23) (a) Mulazzani, Q. G.; Sun, H.; Hoffman, M. Z.; Ford, W. E.; Rodgers, M. A. *J. Phys. Chem.* **1994**, *98*, 1145. (b) Zhang, X.; Rodgers, M. A. *J. Phys. Chem.* **1995**, *99*, 12797.

Table 1. Room Temperature Spectroscopic Data and Energy Transfer Parameters

compound	solvent	$\lambda_{\text{abs max}}$ (nm)	$\lambda_{\text{em max}}$ (nm)	Φ^a	$J (\times 10^{-15},$ $\text{M}^{-1} \text{cm}^{-1})^b$	$R_0 (\text{\AA})^c$
PNI	DMSO	412	544	0.011	13.08	16.1
	CH ₃ CN	406	541	0.076	6.79	23.6
	MeOH	413	545	0.008	5.47	14.2
	EtOH	410	542	0.021	4.34	15.8
	Acetone	402	532	0.148	10.98	23.1
	CH ₂ Cl ₂	413	523	0.904	8.77	32.3
PNI-phen	DMSO	417	544	0.009	13.41	15.7
	CH ₃ CN	412	544	0.042	6.32	20.7
	MeOH	419	547	0.005	4.50	12.7
	EtOH	416	542	0.017	4.55	15.4
	Acetone	407	537	0.072	5.39	18.6
	CH ₂ Cl ₂	418	532	0.801	7.90	31.1

^a Fluorescence quantum yield measured relative to PNI in toluene ($\Phi = 0.91$),^{20a} uncertainty $\pm 10\%$. ^b Spectral overlap integral with a $[\text{Ru}(\text{bpy})_3]^{2+}$ acceptor calculated using Förster theory (see refs 16b, 17, and 18 for details). ^c Calculated Förster distance using a $[\text{Ru}(\text{bpy})_3]^{2+}$ acceptor (see refs 16b, 17, and 18).

corresponding imides, **1** and **3**, preserving the nitro group on the naphthalene. Displacement of the nitro group within **1** and **3** by treatment with excess piperidine in hot DMF yields compounds **2** and **4**, respectively. The dyad and tetrad Ru(II) complexes, $[\text{Ru}(\text{bpy})_2(\text{PNI-phen})](\text{PF}_6)_2$ (**5**) and $[\text{Ru}(\text{PNI-phen})_3](\text{PF}_6)_2$ (**6**), respectively, were prepared using standard procedures, with final purification achieved by chromatography on Sephadex LH-20.

Electrochemistry. The redox behavior of all the compounds in this study was examined by cyclic voltammetry. Both PNI and PNI-phen exhibit reversible one-electron reductions at -1.38 V and -1.31 V vs Ag/AgCl, respectively. The PNI potential is consistent with that obtained in another independent study.^{21a} Under all conditions both PNI and PNI-phen displayed single irreversible oxidations with anodic peaks at $+1.15$ V and $+1.21$ V vs Ag/AgCl, respectively. Using the same experimental apparatus, $[\text{Ru}(\text{bpy})_3]^{2+}$ exhibited the commonly observed single reversible metal-based oxidation at $+1.31$ V vs Ag/AgCl and three reversible ligand-based reductions at -1.31 , -1.49 , and -1.74 V vs Ag/AgCl.²⁴ The dyad, **5**, had a reversible oxidation at $+1.35$ V vs Ag/AgCl and an irreversible anodic peak at $+1.22$ V vs Ag/AgCl. The tetrad, **6**, possessed a reversible wave at $+1.40$ V and an irreversible wave at $+1.17$ V, both vs Ag/AgCl.

Absorption Spectra. The presence of the piperidinyl substituent in the 4-position of the naphthalene-1,8-imide ring generates a chromophore with a lowest energy singlet state of primarily charge-transfer character.²¹ Hence, the absorption band shapes and intensities in the PNI molecules resemble that which is typically observed in MLCT-based chromophores. In addition, the charge-transfer nature of PNI and related molecules imparts a modest degree of solvatochromism in their absorption/emission properties (Table 1). Figure 1 displays the ground-state absorption spectra of $[\text{Ru}(\text{bpy})_3]^{2+}$, PNI-phen, the sum of their spectra, and the dyad $[\text{Ru}(\text{bpy})_2(\text{PNI-phen})]^{2+}$ in CH₃CN. PNI-phen serves as a reference molecule for the naphthalimide chromophore incorporated into the dyad and tetrad complexes. The spectrum of the dyad is well matched by the sum of the spectra of the constituent chromophores. The spectrum of the tetrad is also similar to the sum of its components (not shown). However, the extinction coefficient for the tetrad at 430 nm is 49 400

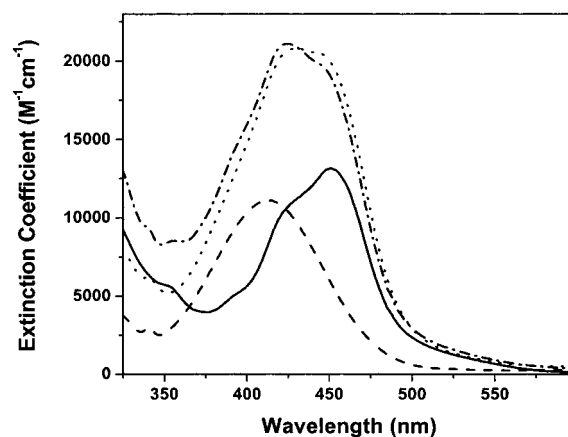


Figure 1. Electronic spectra of $[\text{Ru}(\text{bpy})_3]^{2+}$ (—), PNI-phen (---), and $[\text{Ru}(\text{bpy})_2(\text{PNI-phen})]^{2+}$ (·····) in CH₃CN. The theoretical absorption spectrum of $[\text{Ru}(\text{bpy})_2(\text{PNI-phen})]^{2+}$ (·-·-·) was plotted by adding the electronic spectra of $[\text{Ru}(\text{bpy})_3]^{2+}$ to the spectrum of PNI-phen.

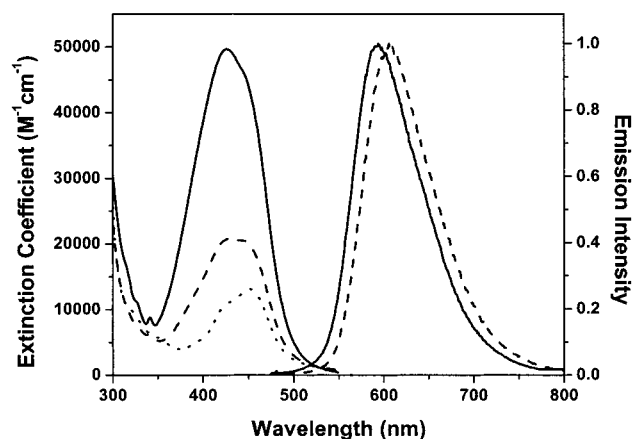


Figure 2. Electronic and uncorrected emission spectra of $[\text{Ru}(\text{bpy})_3]^{2+}$ (·····), $[\text{Ru}(\text{bpy})_2(\text{PNI-phen})]^{2+}$ (---), and $[\text{Ru}(\text{PNI-phen})_3]^{2+}$ (—) in CH₃CN. Emission spectra were measured at 22 °C using 450 nm excitation.

$\text{M}^{-1} \text{cm}^{-1}$, illustrative of the light-harvesting properties of the multiple PNI chromophores (Figure 2). In all cases, covalent attachment does not appear to significantly perturb the charge-transfer transitions in either chromophore. The ground-state absorption spectra of the PNI and $[\text{Ru}(\text{bpy})_3]^{2+}$ units overlap in the molecules where both are present. However, long wavelength excitation (>520 nm) results in negligible excitation ($<5\%$) of the PNI chromophore(s).

Photophysical Properties at Room Temperature. The PNI chromophore has intriguing fluorescence properties that were exploited in the present work to produce *visible* light-harvesting compounds with concomitant long lifetime MLCT-based emission. The overlap integrals and calculated Förster distances for a PNI donor and a $[\text{Ru}(\text{bpy})_3]^{2+}$ acceptor system in a variety of solvents is displayed in Table 1. Even when the donor emission peak is somewhat red-shifted from the MLCT absorption bands, Förster-type singlet energy transfer to $[\text{Ru}(\text{bpy})_3]^{2+}$ is favored in both polar and nonpolar solvents. Both PNI and PNI-phen display singlet fluorescence in a variety of solvents, Table 1. The singlet fluorescence from PNI-phen is nearly quantitatively quenched when chelated to the Ru(II) center in **5** and **6**. The antenna effect of the PNI donor(s) is clearly illustrated by comparing the magnitude of the absorption and excitation spectra in each complex. Figure 3 displays the data obtained

(24) Our values are within experimental error of published values. See: Rillema, D. P.; Allen, G.; Meyer, T. J.; Conrad, D. *Inorg. Chem.* **1983**, *22*, 1617.

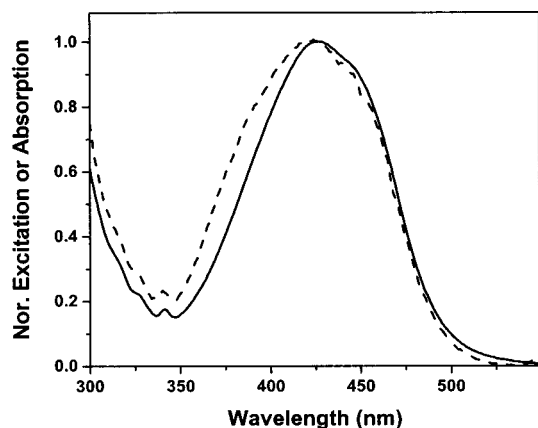


Figure 3. Normalized absorption (—) and corrected excitation (---) spectra of $[\text{Ru}(\text{PNI-phen})_3]^{2+}$ in CH_3CN . Excitation was monitored at 610 nm.

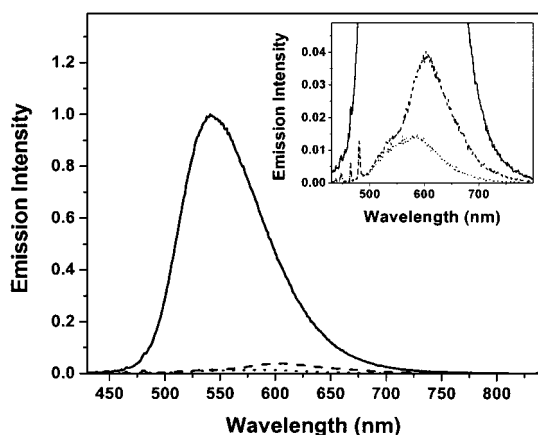


Figure 4. Emission spectra of air-equilibrated, optically matched (0.1 OD, 420 nm) solutions of PNI-phen (—), $[\text{Ru}(\text{bpy})_2(\text{PNI-phen})]^{2+}$ (---), and $[\text{Ru}(\text{PNI-phen})_3]^{2+}$ (.....) measured in CH_3CN with 420 nm excitation. Inset: Close-up view of the emission of $[\text{Ru}(\text{bpy})_2(\text{PNI-phen})]^{2+}$ and $[\text{Ru}(\text{PNI-phen})_3]^{2+}$.

for the tetrad complex. The absorption and the excitation spectra are nearly superimposable, suggesting highly efficient energy transfer from the PNI chromophore(s) to the Ru(II) complex. We were not able to resolve the rise time of the MLCT-based emission following excitation of the PNI chromophore nor were we able to measure the quenched lifetime of the PNI fluorescence ($\tau_0 = 1.21$ ns (PNI) and 0.68 ns (PNI-phen) in CH_3CN) with our TCSPC lifetime apparatus, providing further evidence for rapid and efficient energy transfer.^{11,16,25} In air-equilibrated solvents, the residual, dioxygen insensitive singlet fluorescence from the PNI unit(s) is observed as a high-energy shoulder in the emission spectra of **5** and **6**, Figure 4. Figure 4 illustrates the strong quenching of the singlet PNI fluorescence in the two complexes.

The MLCT-based emission in **5** and **6** is dynamically quenched by dioxygen in all solvents investigated. The k_q values for dioxygen quenching in CH_3CN are $6.0 \times 10^8 \text{ M}^{-1}\text{s}^{-1}$ and $7.2 \times 10^8 \text{ M}^{-1}\text{s}^{-1}$ for **5** and **6**, respectively. Table 2 displays the photophysical data of compounds **5** and **6** obtained in a variety of solvents. In all cases, the lifetimes of the tetrad are 2–3 times that of the dyad in each solvent investigated. The excited-state lifetimes exhibited by **5** and **6** are notably longer than those displayed by their respective model complexes.

Since the emission lifetimes of the dyad and tetrad are quite long relative to the model MLCT complexes, the values of η_{isc} k_t calculated for **5** and **6** are on the order of $\sim 10^3 \text{ s}^{-1}$ and $\sim 10^2$

s^{-1} , respectively (Table 2). These values are significantly smaller than that typically attributed to MLCT compounds with η_{isc} values of unity (10^5 s^{-1}).^{1,9} The small values of η_{isc} k_t for **5** and **6** are inconsistent with that expected for “normal” Ru(II) MLCT complexes and the intervening triplet states on the PNI-containing ligand(s) are presumed responsible for this behavior.

Pulsed laser excitation at wavelengths between 355 and 550 nm generates MLCT-based emission centered near 600 nm in both **5** and **6** (Figure 2), displaying complex decay kinetics. Generally a fast component is always observed within our instrument response (< 15 ns) that is in part due to the tail of the residual singlet fluorescence of PNI. Control studies reveal that this fluorescence does not completely account for the observed fast component. In all solvents, the long decay component comprises the major fraction of the decay, and under conditions where the oscilloscope does not sample the fast component, single-exponential kinetics were observed on time scales adequate to measure the full recovery of the ground state. There was no evidence for distinct microsecond decay components resembling that expected for $[\text{Ru}(\text{bpy})_3]^{2+}$, $[\text{Ru}(\text{bpy})_2(\text{phen})]^{2+}$, or $[\text{Ru}(\text{phen})_3]^{2+}$. Table 2 summarizes the emission lifetimes displayed by the complexes obtained by sampling only the long decay component. Time-resolved emission spectra performed at room temperature confirmed a single emission band emerging from both complexes at all delay times.

The transient absorption spectra of the PNI model **2** and PNI-phen **4** following a 355 nm laser pulse are identical within experimental error. In both cases the transients are very weak; however, using the triplet sensitizer thioxanthone,²⁶ the intensity of these transients markedly increased. For brevity, Figure 5a presents the data obtained for PNI-phen in CH_3CN , using a sufficient delay time (20 μs) to suppress the thioxanthone sensitizer transients. On the basis of the fact that the spectra were easily triplet sensitized, displayed lifetimes on the order of 45 μs in CH_3CN ,²⁷ and were extremely sensitive to dioxygen, the transient features were assigned to ^3PNI and $^3\text{PNI-phen}$. In addition, the electron donor DABCO was able to react with both of these triplet states via electron transfer, producing the radical anion of PNI ($\text{PNI}^{\cdot-}$) as depicted in eq 1.



The transient spectrum of $\text{PNI}^{\cdot-}$ resulting from the reduction of the triplet state of PNI^* is presented in Supporting Information. The radical anion spectrum of PNI was strikingly similar to the radical anions produced from other naphthalimide chromophores.^{28,29}

The excited-state absorption spectra of the dyad and tetrad following either 355 or 532 nm excitation generated transients consistent with that assigned to ^3PNI and $^3\text{PNI-phen}$, indicating that the excitation is predominately localized on the PNI unit(s). The rise time of the triplet-triplet absorption spectrum could not be resolved with our instrumentation (< 15 ns), indicating that the ^3PNI is likely sensitized through rapid

(25) (a) Bignozzi, C. A.; Roffia, S.; Chiorboli, C.; Davila, J.; Indelli, M. T.; Scandola, F. *Inorg. Chem.* **1989**, *28*, 4350. (b) Amadelli, R.; Argazzi, R.; Bignozzi, C. A.; Scandola, F. *J. Am. Chem. Soc.* **1990**, *112*, 7099.

(26) Rogers, J. E.; Kelly, L. A. *J. Am. Chem. Soc.* **1999**, *121*, 3854.

(27) In CH_3CN solutions the decay kinetics of the PNI triplet state was complex, except in extremely dilute solutions using low laser fluence at 355 nm where the decay becomes nearly monoexponential.

(28) Aveline, B. M.; Matsugo, S.; Redmond, R. W. *J. Am. Chem. Soc.* **1997**, *119*, 11785.

(29) Demeter, A.; Biczók, L.; Bérces, T.; Wintgens, V.; Valat, P.; Kossanyi, J. *J. Phys. Chem.* **1993**, *97*, 3217.

Table 2. Spectroscopic and Photophysical Data for **5** and **6** at Room Temperature

compound	solvent	$\lambda_{\text{abs max}}^a$ (nm)	$\lambda_{\text{em max}}$ (nm)	$\tau_{\text{em, TRPL}}^b$ (μs)	τ, TA^c (μs)	Φ_{em}^d	$\eta_{\text{isc}k_r}^e$ (s^{-1})	k_{nr} (s^{-1})	intensity quenching ^f
[Ru(bpy) ₂ (PNI-phen)] ²⁺	DMSO	436	617	46.68	43.34	0.057	1.32×10^3	2.18×10^4	92.6%
	CH ₃ CN	430	606	27.60	24.67	0.033	1.20×10^3	3.52×10^4	98.7%
	MeOH	446	605	33.78	32.17	0.038	1.12×10^3	2.84×10^4	96.3%
	EtOH	446	601	40.17	37.78	0.033	0.82×10^3	2.41×10^4	98.1%
	Acetone	426	607	16.27	17.21	0.055	3.38×10^3	5.81×10^4	98.8%
	CH ₂ Cl ₂	449	590	36.81	36.63	0.025	0.68×10^3	2.65×10^4	98.7%
[Ru(PNI-phen) ₃] ²⁺	DMSO	435	605	115.09	114.85	0.032	2.78×10^2	8.41×10^4	92.5%
	CH ₃ CN	427	595	60.80	61.53	0.013	2.14×10^2	1.43×10^4	99.0%
	MeOH	432	593	73.34	67.10	0.023	3.13×10^2	1.33×10^4	93.4%
	EtOH	435	590	103.60	101.60	0.017	1.64×10^2	0.95×10^4	98.4%
	Acetone	422	595	43.13	42.04	0.022	5.10×10^2	2.27×10^4	98.4%
	CH ₂ Cl ₂	447	573	68.68	65.46	0.005	0.72×10^2	1.43×10^4	99.6%

^a Absorption spectra were broad in all solvents. ^b Emission lifetimes represent an average of at least five measurements and have an uncertainty of less than 10%. Here the data were obtained using 458 ± 2 nm excitation. ^c The lifetime of the triplet-triplet PNI absorption, measured near 470 nm with 355 nm excitation. ^d Photoluminescence quantum yield using [Ru(bpy)₃]²⁺ ($\Phi = 0.062$)²² in CH₃CN as the quantum counter, $\pm 10\%$. ^e Calculated from the expression: $\Phi_{\text{em}}/\tau_{\text{em}} = \eta_{\text{isc}k_r}$. ^f Intensity quenching of the singlet PNI-phen fluorescence using optically matched solutions (OD = 0.1 at 420 nm) of PNI-phen and the appropriate metal complex.

triplet-triplet energy transfer from the MLCT fragment. The decay kinetics of these absorption transients closely parallel the values independently obtained from time-resolved emission measurements in all solvents studied (Table 2), suggesting that the two processes are intimately coupled. Similarly, dynamic quenching of the MLCT-based luminescence by the addition of dioxygen quenches the ³PNI absorption transients to the same extent.

Photophysical Properties at 77 K. PNI and PNI-phen do not display any measurable phosphorescence in frozen glasses at 77 K even with the addition of ethyl iodide. The steady state 77 K emission spectra of [Ru(bpy)₂(PNI-phen)]²⁺ and [Ru(bpy)₂(phen)]²⁺ (for comparison) are displayed in Figure 6a. The spectrum of the dyad and [Ru(bpy)₂(phen)]²⁺ are quite similar in energy and band shape, except at lower energy where the vibrational features are more pronounced in the dyad. In both complexes, we measured the emission spectra as a function of excitation wavelength ($\lambda_{\text{ex}} = 390, 420, 450, 470,$ and 500 nm)³⁰ as well as the excitation spectra as a function of emission wavelength ($\lambda_{\text{em}} = 580$ and 620 nm).³¹ In all cases, the resulting normalized spectra were identical within experimental error. These data indicate that the same ratio of MLCT to ligand triplet states is formed independent of excitation wavelength.

In an attempt to separate the components comprising the 77 K spectrum, we measured the time-resolved emission spectrum of [Ru(bpy)₂(PNI-phen)]²⁺ (Figure 6b and c). Figure 6b presents the emission spectrum obtained 500 ns after a 458 nm, 500 ps laser pulse. This particular spectrum decays with complex kinetics but possesses a long lifetime component of 3.7 μs , shorter than the single-exponential lifetime observed for [Ru(bpy)₂(phen)]²⁺ in the same matrix (6.35 μs). Figure 6c displays the emission spectrum generated 20 μs after a 458 nm, 500 ps laser pulse. The decay of this spectrum is complex, containing a long-lifetime component tailing into the millisecond regime, consistent with that typically observed for triplet phosphorescence. We believe the latter reveals the phosphorescence spectrum of the ³PNI when covalently attached to the metal complex. These data permit direct evaluation of the E₀₋₀ triplet levels of the ³PNI unit (16 650 cm⁻¹) and the ³MLCT fragment (17 400 cm⁻¹), without the need for model systems. This was a key result since the ³PNI level would have been difficult to

determine in the absence of the time-resolved emission data. Quite unlike that observed in the room-temperature experiments, the shorter-lived components in the dyad comprises the majority of the intensity decay at 77 K, suggesting minimal population of the ³PNI species at low temperature. Similar behavior was observed in the 77 K time-resolved emission spectrum of **6**, and the strong ³MLCT emission band centered at 570 nm (17 544 cm⁻¹) was consistent with that expected for [Ru(phen)₃]²⁺. In this case, however, the long wavelength phosphorescence spectrum could not be resolved.

Discussion

Electrochemistry. Compounds **5** and **6** displayed oxidative behavior consistent with that expected for the sum of the components. The more positive oxidations were attributed to the metal-centered reaction Ru(II) \rightarrow Ru(III). In each case the PNI-based oxidation was observed at a potential slightly negative of the metal-based oxidation. In CH₃CN and DMF, the successive ligand-based reduction waves were difficult to visualize in both **5** and **6**, likely due to irreversible chemistry on the PNI unit(s). No attempts were made to further investigate these reductive processes.

Absorption and Electronic Properties. The present study demonstrates that it is indeed feasible to generate visible light-harvesting metal-organic compounds that display unusually long MLCT-based emission lifetimes at room temperature. The synthetically versatile PNI chromophore was readily incorporated into a 1,10-phenanthroline ligand, then chelated to two Ru(II) complexes using standard procedures (Scheme 1). Molecular modeling of the PNI-phen ligand using Spartan 5.0 (MMFF94)³² revealed that the C-N bond connecting the phenanthroline and PNI portions of the molecule is twisted by 59° (Figure 7), a value consistent with that observed for PNI similarly attached to substituted benzenes.³³ From this modeling data, the calculated center-to-center distance from the PNI unit to the MLCT core was 9.5 Å. The nonplanar structure is expected to substantially reduce the electronic coupling between the MLCT core and the PNI unit(s) in both metal complexes under investigation.¹⁴ Therefore, it is not surprising that the data presented for the dyad in Figure 1 represents the sum of the individual chromophores that comprise the molecule.

(30) Reitz, G. A.; Demas, J. N.; DeGraff, B. A.; Stephens, E. M. *J. Am. Chem. Soc.* **1988**, *110*, 5051.

(31) Sacksteder, L. A.; Lee, M.; Demas, J. N.; DeGraff, B. A. *J. Am. Chem. Soc.* **1993**, *115*, 8230.

(32) Halgren, T. A. *J. Comput. Chem.* **1996**, *17*, 490.

(33) (a) Lukas, A. S.; Miller, S. E.; Wasielewski, M. R. *J. Phys. Chem. B* **2000**, *104*, 931. (b) Miller, S. E.; Lukas, A. S.; Marsh, E.; Bushard, P.; Wasielewski, M. R. *J. Am. Chem. Soc.* **2000**, *122*, 7802.

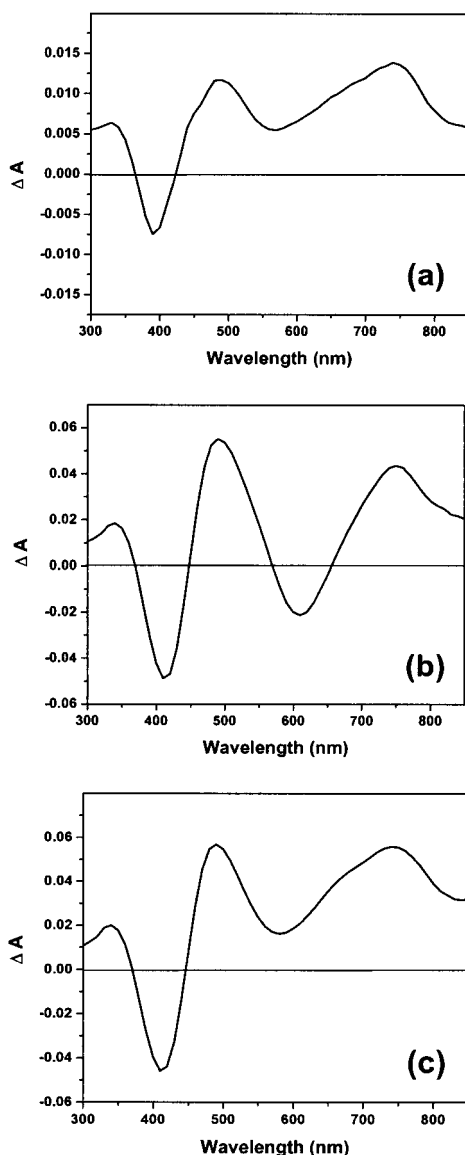


Figure 5. Excited-state absorption difference spectra for (a) PNI-phen, (b) $[\text{Ru}(\text{bpy})_2(\text{PNI-phen})]^{2+}$, and (c) $[\text{Ru}(\text{PNI-phen})_3]^{2+}$ in CH_3CN following 355 nm pulsed excitation. Spectrum (a) was collected 20 μs after the laser pulse ensuring significant disappearance of the thioxanthone sensitizer transients. Spectra (b) and (c) were obtained 2 μs after the laser pulse and displayed similar transient features at all time intervals.

Light-Harvesting and Energy Transfer. The PNI chromophore(s) provides an antenna system for the efficient harvesting of visible light. The energy transfer efficiency from the PNI chromophore(s) to the MLCT fragment, calculated by comparing the relative magnitude of the absorption and excitation spectra, was greater than 92% in all solvents investigated, see Figures 3 and 4 and Table 2. This is not surprising given the close proximity (9.5 Å) of the two chromophores, Figure 7. The present work does not reveal a specific mechanism for the efficient population of the MLCT emissive states through excitation of ^1PNI . However, a plausible mechanism is Förster-type singlet energy transfer as the critical distances in each solvent (Table 1) favor these processes. Previous work from our laboratory has demonstrated that Förster-type singlet energy transfer (from coumarin 460) can efficiently sensitize the MLCT excited states in $[\text{Ru}(\text{bpy})_3]^{2+}$.^{16b} However, the PNI chromophores in the present work possess other intervening states

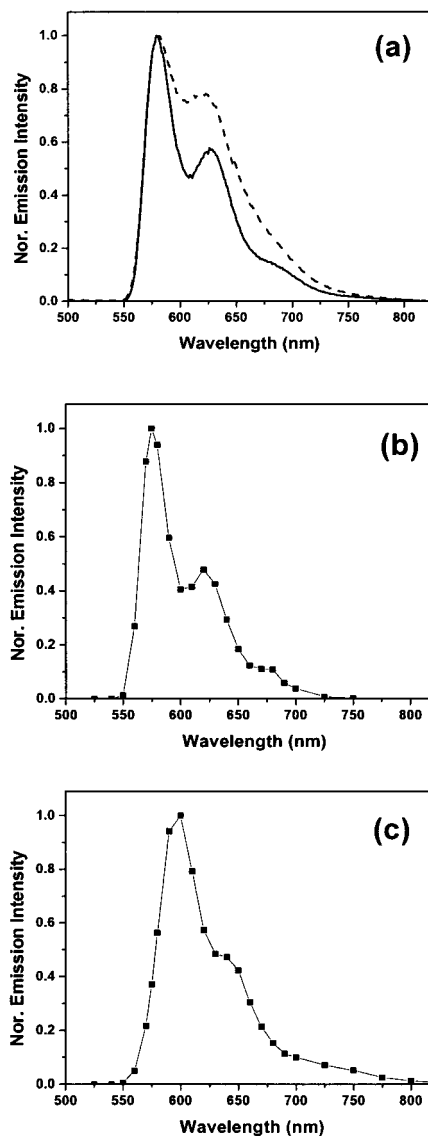


Figure 6. (a) 77 K emission spectra of $[\text{Ru}(\text{bpy})_2(\text{phen})]^{2+}$ (—) and $[\text{Ru}(\text{bpy})_2(\text{PNI-phen})]^{2+}$ (---) in 4:1 ethanol/methanol with 450 nm excitation. (b) 77 K emission spectrum of $[\text{Ru}(\text{bpy})_2(\text{PNI-phen})]^{2+}$ measured 0.5 μs after a 458 nm laser pulse. (c) 77 K emission spectrum of $[\text{Ru}(\text{bpy})_2(\text{PNI-phen})]^{2+}$ measured 20 μs after a 458 nm laser pulse.

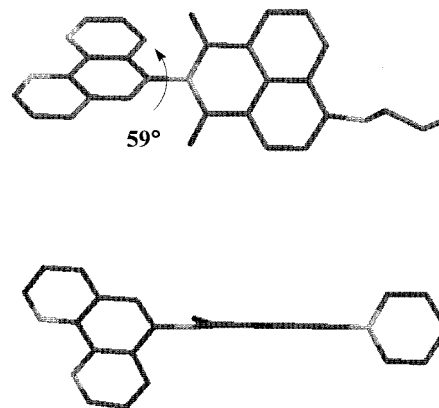


Figure 7. Molecular models of PNI-phen calculated using Spartan 5.0 (MMFF94). The C-N bond connecting the phenanthroline and PNI unit is twisted by 59°.

and alternative pathways exist that could result in the above experimental observations (Figure 8).

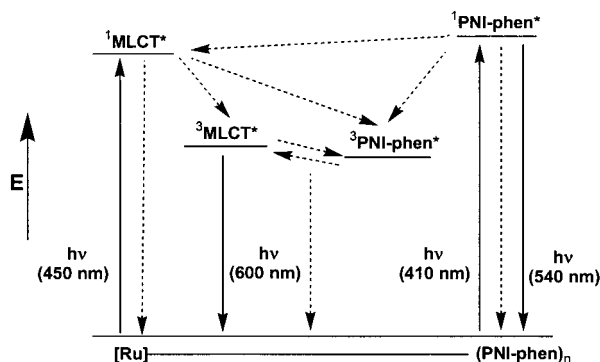


Figure 8. Energy level diagram describing the photophysical processes of $[\text{Ru}(\text{bpy})_2(\text{PNI-phen})]^{2+}$ and $[\text{Ru}(\text{PNI-phen})_3]^{2+}$. Solid lines represent radiative transitions and dashed lines represent nonradiative transitions.

Nature of the Excited States. The time-resolved emission spectra obtained at 77 K (Figure 6) permits the separation of the multiple emissions emerging from the complexes in this study. These observations are not unique as there are many examples of MLCT compounds, where in low-temperature rigid glasses, multiple luminescences are observed. Some of these include the MLCT compounds of DeArmond (Rh(III)),³⁴ Watts (Ir(III)),³⁵ Wrighton (Re(I)),³⁶ Demas (Re(I)),^{30,31} and McMillan (Cu(I)).³⁷ Although there are several examples of Ru(II) MLCT complexes containing multiple excited states,^{9,15} dual emissions are generally not observed in these species. If only low-temperature steady-state data (excitation and emission spectra) were relied upon in the present work, we would have concluded that one excited state was present at 77 K. However, our low-temperature time-resolved data clearly indicated an inhomogeneous population of emitting species.

Demas and co-workers observed similar photophysical phenomena in Re(I) isocyanate complexes and used a three-level excited-state model to describe the temperature dependence of the luminescence.³¹ Our inability to perform such measurements prompted us to evaluate the time-resolved emission spectra at 77 K (Figure 6) in order to separate the ³MLCT and ³PNI emitting components. These data permit the construction of an energy level diagram depicting the relative energy levels within the dyad and tetrad, Figure 8. Presuming that the lower energy phosphorescence emerges from ³PNI, the ³MLCT level is approximately 750 and 900 cm^{-1} above the ³PNI levels in **5** and **6**, respectively. On the basis of the relative energies of the two triplet levels, the room-temperature experimental data are consistent with an excited-state equilibrium established between the ³MLCT and the ³PNI fragments.

The transient absorption data reveals the prompt appearance of the ³PNI species following excitation of the MLCT fragment on the nanoseconds time scale (Figure 6) in both compounds in all solvents investigated. At all delay times, no characteristic

³MLCT transient absorption signatures could be detected, suggesting that the excited state is predominately localized on the PNI unit(s), consistent with that suggested by the luminescence ($\eta_{\text{isc}}k_{\text{r}}$ and lifetime) data. The large intensity of the transients in the dyad and tetrad indicate that they are likely sensitized by triplet-triplet energy transfer from the ³MLCT excited states. This is supported by the observation of a short-lived component in the MLCT emission at room temperature, consistent with a fast energy transfer process. Similarly, the time-resolved emission data obtained at 77 K also reveals a shorter lived MLCT-based emission than one would expect given the lifetimes of the model complexes, also consistent with triplet energy transfer. Alternatively, it is possible that the ³PNI states could be accessed through direct intersystem crossing from the ¹MLCT excited states (Figure 8). Ultrafast transient absorption spectroscopy would be particularly valuable in discerning the processes leading to thermal equilibrium in these complexes and we are presently exploring this possibility.

In all deaerated solvents, the decay of the ³PNI transient absorptions follow the same kinetics as the MLCT-based emission in the dyad and tetrad. The fact that the ³MLCT emissive states are populated and decay at the same rate as the absorption transients assigned to ³PNI suggests that the two triplets are in equilibrium, consistent with that previously observed in a number of Ru(II)-pyrene systems.¹⁰⁻¹³

The excited-state lifetimes of **6** are always 2-3 times greater than those observed for **5**. These data suggest that the presence of 3 PNI units has the effect of driving the equilibrium toward ³PNI, in turn extending the lifetimes observed in the tetrad relative to the dyad. In other words, **6** displays more "PNI-like" character than **5**, as there are 3 PNI chromophores relative to 1 which to distribute the excitation. Our group has recently observed a similar phenomenon in Ru(II)-diimine complexes containing multiple pyrenyl chromophores.¹³ The equilibrium in the present work will also be influenced by the energy gap between the ³MLCT and ³PNI states, which is slightly larger (150 cm^{-1}) in the tetrad relative to the dyad. Small changes in these energies can markedly affect their relative populations and, thus, the emission properties.³¹

Solvent Effects. The extreme solvent sensitivity of the excited states produced in the dyad and tetrad can be likely attributed to the charge-transfer character exhibited by both the PNI and $[\text{Ru}(\text{L-L})_3]^{2+}$ -like core. Interestingly, the observed lifetimes do not follow any clear trend in terms of solvent properties such as dielectric constant or acceptor number. Above we have presented a generalized case in which our data can be broadly interpreted. However, solvent interactions can perturbate the electronic properties of the complexes. We believe that the solvent must be directly influencing the equilibrium process in order to account for the wide variation in observed lifetimes. Most likely, solvent-induced changes in the ³MLCT and ³PNI energy levels influences their relative populations, which markedly impacts the observed luminescence properties. These solvent effects presently remain under investigation.

Conclusions

This study demonstrates that proper selection of organic chromophores with appropriate singlet and triplet energies can generate visible light-harvesting Ru(II) MLCT complexes that display extended excited-state lifetimes. PNI singlet states were used as light-harvesting antennae to sensitize an excited-state manifold composed of both ³MLCT and ³PNI states. Once formed, the sensitized triplet states attain thermal equilibrium at room temperature as both species can be independently

(34) Halper, W.; DeArmond, M. K. *J. Lumin.* **1972**, *5*, 225.

(35) (a) Watts, R. J.; Brown, M. J.; Griffith, B. G.; Harrington, J. S. *J. Am. Chem. Soc.* **1975**, *97*, 6029. (b) Watts, R. J.; Griffith, B. G.; Harrington, J. S. *J. Am. Chem. Soc.* **1976**, *98*, 674.

(36) (a) Wrighton, M. S.; Morse, D. L. *J. Am. Chem. Soc.* **1974**, *96*, 998. (b) Luong, J. C.; Faltynak, R. H.; Wrighton, M. S. *J. Am. Chem. Soc.* **1979**, *101*, 1597. (c) Fredericks, S. M.; Luong, J. C.; Wrighton, M. S. *J. Am. Chem. Soc.* **1979**, *101*, 7415. (d) Giordano, P. J.; Wrighton, M. S. *J. Am. Chem. Soc.* **1979**, *101*, 2888.

(37) (a) Rader, R. A.; McMillin, D. R.; Buckner, M. T.; Matthews, T. G.; Casadonte, D. J.; Lengel, R. K.; Whittaker, S. B.; Darmon, L. M.; Lytle, F. E. *J. Am. Chem. Soc.* **1981**, *103*, 5906. (b) Kirchoff, J. R.; Gamache, R. E., Jr.; Blaskie, M. W.; Del Paggio, A. A.; Lengel, R. K.; McMillin, D. R. *Inorg. Chem.* **1983**, *22*, 2380.

monitored using time-resolved absorption and emission spectroscopy. This thermal equilibrium is lifted at 77 K as dual luminescence from each triplet state could be observed in the time-resolved emission spectra of the metal complexes. The low-temperature data permitted the construction of energy level diagram, depicting each participant in the excited-state manifold. The observed lifetimes are sensitive to the number of PNI chromophores within the molecule, suggesting that the excited-state equilibrium (and observed lifetime) is synthetically tunable. The room temperature excited-state lifetimes in both complexes were extremely sensitive to solvent and could be tuned over a

broad range (16 to 115 μs). Luminophores exhibiting such unique photophysical properties will undoubtedly be valuable for applications in emerging fluorescence technologies.

Acknowledgment. D.S.T. was supported by a G. S. Hammond Fellowship of the McMaster Endowment administered by the Center for Photochemical Sciences at BGSU.

Supporting Information Available: Excitation and emission spectra for **5** and the transient spectrum of the radical anion of PNI are presented.

IC010287G